

# Do high-velocity clouds form by thermal instability?

James Binney<sup>1\*</sup>, Carlo Nipoti<sup>2</sup> and Filippo Fraternali<sup>2</sup>

<sup>1</sup> *Rudolf Peierls Centre for Theoretical Physics, Keble Road, Oxford OX1 3NP, UK*

<sup>2</sup> *Dipartimento di Astronomia, Università di Bologna, via Ranzani 1, 40127 Bologna, Italy*

Accepted 2009 May 20. Received 2009 May 15; in original form 2009 February 25

## ABSTRACT

We examine the proposal that the H I “high-velocity” clouds (HVCs) surrounding the Milky Way and other disc galaxies form by condensation of the hot galactic corona via thermal instability. Under the assumption that the galactic corona is well represented by a non-rotating, stratified atmosphere, we find that for this formation mechanism to work the corona must have an almost perfectly flat entropy profile. In all other cases the growth of thermal perturbations is suppressed by a combination of buoyancy and thermal conduction. Even if the entropy profile were nearly flat, cold clouds with sizes smaller than 10 kpc could form in the corona of the Milky Way only at radii larger than 100 kpc, in contradiction with the determined distances of the largest HVC complexes. Clouds with sizes of a few kpc can form in the inner halo only in low-mass systems. We conclude that unless even slow rotation qualitatively changes the dynamics of a corona, thermal instability is unlikely to be a viable mechanism for formation of cold clouds around disc galaxies.

**Key words:** ISM: kinematics and dynamics, galaxies: haloes, galaxies: kinematics and dynamics, galaxies: evolution

## 1 INTRODUCTION

It is widely accepted that star-forming disc galaxies such as the Milky Way have sustained their star formation over gigayears by accreting gas at a fairly steady or slowly declining rate (e.g. Chiappini, Matteucci & Romano 2001). The source of this gas is uncertain. The Milky Way and other star-forming disc galaxies (such as M31) that have been studied with sufficient sensitivity in the 21-cm hyperfine-structure line of hydrogen are surrounded by clouds of H I (e.g. Wakker & van Woerden 1997; Westmeier, Braun & Thilker 2005), but the amount of gas contained in these “high-velocity” clouds (HVCs) is sufficient to sustain accretion onto the disc for about a gigayear (e.g. Wakker et al. 2007; Sancisi et al. 2008). The only realistic source of gas for sustained accretion onto discs is the warm-hot intergalactic medium (WHIM), which is believed to contain over half the baryons in the Universe. This belief is based on a combination of big-bang nucleosynthesis theory and observations of the cosmic microwave background (e.g. Fukugita, Hogan & Peebles 1998), so within the framework of standard cosmology it must be considered robust. Empirical evidence for the existence of the WHIM includes the requirement for a medium to confine clouds of interstellar gas far from the Galactic plane (Spitzer 1956), the observation of CIV, OV

and OVI absorption along lines of sight that pass close to the Galaxy’s HVCs (Sembach et al. 2003; Fox, Savage & Wakker 2006), and the morphology of the Magellanic Stream and individual HVCs (Putman et al. 2003; Brüns et al. 2000).

The relationship of the WHIM to circum-galactic clouds of H I is unclear. Undoubtedly much of the H I that is observed more than a kiloparsec from galactic planes has been pushed off the star-forming plane by the mechanical feedback from star formation (e.g. Fraternali & Binney 2008) – the galactic fountain effect (Shapiro & Field 1976). Bregman (1980) proposed that the galactic fountain model could explain also the formation of the HVCs by condensation from hot gas outflows from the disk, but Ferrara & Einaudi (1992) argued on theoretical grounds that this mechanism is unlikely to work. The hypothesis that HVCs formed by condensation of the hot gas of the galactic fountain is discarded also on observational grounds, because such gas cannot be less metal rich than the local interstellar medium, whereas the high-velocity cloud Complex C, which lies 6 – 11 kpc from the plane, has  $Z \simeq 0.15Z_{\odot}$  (Wakker et al. 2007). This finding suggests that some HVCs, especially those more than  $\sim 5$  kpc from the plane, represent matter that is entering the Galaxy for the first time (Oort 1970).

At least some HVCs must have been stripped from infalling satellites because some clouds are clearly associated with the Magellanic Stream, which is itself thought to have been torn from the Small Magellanic Cloud (Putman et al.

\* E-mail: binney@thphys.ox.ac.uk

2003). Counts of stars in the Sloan Digital Sky Survey (Bell et al. 2008) and in deep surveys of M31 (Richardson et al. 2008) have shown that the outer stellar halos of the Galaxy and M31 are far from relaxed and are best thought of as a superpositions of dissolving satellites. Any gas that belonged to these satellites is likely to give rise to HVCs.

However, the supply of cold gas from infalling satellites falls far short of what a typical star-forming disc galaxy needs to sustain its star formation (e.g. Sancisi et al. 2008). In the long run that gas *must* come from the WHIM because the latter is the only gas reservoir of sufficient capacity. So if star-forming galaxies obtain the gas they need by accreting HVCs, these clouds must form from the WHIM. A case for the formation of HVCs from the WHIM has been argued on the basis of simulations of galaxy formation that follow the baryons with SPH (Kaufmann et al. 2006; Sommer-Larsen 2006; Peek, Putman & Sommer-Larsen 2008; Kaufmann et al. 2009). This case is not strong because (a) the mass scale of HVCs is smaller than the mass resolution of state of the art cosmological simulations, (b) there are grave doubts about the reliability of SPH when the fluid contains extremely steep density gradients such as those expected at the interface of the WHIM and an H I cloud and (c) multi-phase media in SPH simulations might be subject to artificial overcooling (Marri & White 2003; Kaufmann et al. 2007; Agertz et al. 2007, but see also Price 2008). In this paper we use largely analytic arguments to examine the likelihood that H I clouds can condense from the WHIM  $\gtrsim 10$  kpc above the main H I disc.

The dynamics of the WHIM around a galaxy such as the Milky Way bears a close resemblance to the dynamics of “cooling flows” in groups and clusters of galaxies. The gas in a cooling flow is hotter and denser than the WHIM, so it can be readily studied through its X-ray emission. When observations showed that the cooling time at the centre of a typical cooling flow is significantly less than the Hubble time, it was assumed that the gas was flowing towards the centre and there generating a pool of cold gas from which stars formed (Silk 1976; Cowie & Binney 1977). Shortly afterwards it became clear that this picture was not viable because (a) it predicted a radial X-ray surface-brightness profile that was too centrally concentrated, and (b) insufficient young stars were present at small radii, no matter what the initial mass function. The hypothesis then took firm root that  $\sim 100$  kpc from the centre, thermal instability in the inflowing gas caused clouds of cold gas to “drop out” (Nulsen 1986). These clouds were presumed to be too small to be detected, but removed sufficient X-ray emitting gas from the cooling flow to reconcile the theoretical and observational surface-brightness profiles. Eventually this theory of “distributed mass drop out” was ruled out by the absence of spectral lines in soft X-rays that should have accompanied the formation of the clouds (Peterson et al. 2002). However, more than a decade before the decisive observational evidence arrived the intellectual foundations of the theory had been shot away by Malagoli, Rosner & Bodo (1987, hereafter MRB), who pointed out that a hot atmosphere that is confined by a gravitational field and radially stratified by specific entropy is not thermally unstable in the sense of Field (1965). Subsequent papers clarified important aspects of the problem (Balbus & Soker 1989, hereafter BS, Tribble 1989; Balbus 1991) but confirmed the basic physical prin-

ciple. Unfortunately, it seems that the community that is now working on galaxy formation is unaware of this principle (e.g. Maller & Bullock 2004, Peek et al. 2008), and there is a danger that studies of the WHIM will fall into the same trap as did early studies of cooling flows. In particular, condensation of the WHIM into HVCs  $\gtrsim 10$  kpc above the H I disc is an instance of distributed mass drop out, albeit in a different parameter regime. In this paper we examine this possibility critically.

In Section 2 we summarise the analytical work of MRB and BS, and explain the underlying physics. In Section 3 we describe the simple models of galactic coronae in which we study thermal instability. Section 4 presents both the result of applying linear theory to these models and studying the time evolution of spherical model atmospheres. Section 5 sums up and discusses the implications of our results for galaxy accretion.

## 2 THERMAL INSTABILITY IN STRATIFIED CORONAE

The WHIM around a galaxy like the Milky Way is expected to be approximately in equilibrium, stratified in the galactic gravitational potential. The thermal instability in gravitationally stratified coronae has been studied by several authors (e.g. MRB, White & Sarazin 1987; Tribble 1989, BS), mainly in the context of the study of cooling flows in galaxy clusters. In many respects a galactic corona is just a scaled-down version of the hot atmosphere of a galaxy cluster. Thus, under the assumption that the corona is non-rotating and spherically symmetric, the formalism of previous work of spherical models of cooling flows can be applied straightforwardly. However, the detailed thermal behaviour of the system is sensitive to the gas temperature and density distribution, so the conclusions drawn in the case of clusters cannot be a priori extended to lower-mass systems.

Here we follow the treatment of MRB who used Eulerian plane-wave perturbations to study thermal instability in a spherically symmetric stratified atmosphere in the presence of a flow, including the effects of cooling and thermal conduction. It has been pointed out that when a background flow is present, the use of Lagrangian perturbations is preferable to that of Eulerian perturbations (Balbus 1988; Tribble 1989, BS). However, the main results of MRB have been confirmed by the Lagrangian study of BS. Thus, for the purpose of the present investigation we prefer to use the Eulerian approach, which has the advantage of a simpler formalism than the Lagrangian approach.

### 2.1 Perturbation analysis

We summarise here the perturbation analysis of a non-rotating spherical stratified atmosphere by MRB. The system is governed by the equations for mass, momentum and energy conservation

$$\frac{\partial \rho}{\partial t} + \nabla \cdot (\rho \mathbf{v}) = 0, \quad (1)$$

$$\frac{\partial \mathbf{v}}{\partial t} + \mathbf{v} \cdot \nabla \mathbf{v} = -\frac{\nabla p}{\rho} - \nabla \Phi, \quad (2)$$

$$\frac{p}{\gamma - 1} \left[ \frac{\partial}{\partial t} + \mathbf{v} \cdot \nabla \right] \ln(p\rho^{-\gamma}) = \nabla \cdot (f_{\kappa} T^{5/2} \nabla T)$$

$$-\left(\frac{\rho}{\mu m_p}\right)^2 \Lambda(T). \quad (3)$$

Here  $\Phi$  is the galactic gravitational potential,  $\gamma = 5/3$  is the ratio of principal specific heats,  $\Lambda$  is the cooling function,  $\mu$  is the mean gas particle mass in units of the proton mass  $m_p$ ,  $\kappa_S \simeq 1.84 \times 10^{-5} \text{ erg s}^{-1} \text{ cm}^{-1} \text{ K}^{-7/2}$  is Spitzer's coefficient of thermal conductivity (assuming a value 30 for the Coulomb logarithm; Spitzer 1962) and  $f \leq 1$  is the factor by which thermal conduction is suppressed by a tangled magnetic field (e.g. Binney & Cowie 1981). We are assuming that the thermal conductivity is unsaturated, which will certainly be the case in an isothermal corona since there the only temperature gradients are those associated with perturbations and therefore of order  $\delta T/\lambda$ , where  $\delta T$  is infinitesimal and  $\lambda$  is the perturbation's wavelength. Near the edge of an adiabatic corona the temperature gradient is steep and the density low (Fig. 5 below), so the conductivity may saturate. Reduced conductivity will underline the tendency of these regions to be thermally unstable.

Apart from the presence of the factor  $f$ , we treat the hot galactic gas as unmagnetized. We do not attempt to model the magnetic field in the corona for simplicity and because its properties are poorly constrained. An ordered magnetic field can have subtle effects on thermal instability (Loewenstein 1990; Balbus 1991), but, as we explain in Section 5, far from the disc the field is unlikely to be ordered.

The unperturbed corona is assumed to be close to hydrostatic and thermal equilibrium in the sense that the system is approximately in a steady state over the time scales of interest even in the presence of radiative cooling and thermal conduction. Thus, the corona can be described by the time-independent spherically-symmetric pressure  $p$ , density  $\rho$ , temperature  $T$  and velocity field  $\mathbf{v} = v\mathbf{e}_r$ , which satisfy equations (1) to (3) with vanishing partial derivatives with respect to  $t$ .

We linearise equations (1-3) with Eulerian perturbations of the form  $F + \delta F \exp(-i\omega t + ik_r r + i\mathbf{k}_t \cdot \mathbf{x}_t)$ , where  $\mathbf{x}_t$  is the tangential vector,  $k_r$  is the radial wave-number,  $k_t \equiv |\mathbf{k}_t|$  is the tangential wave-number and  $|\delta F| \ll |F|$ . Under the assumption of short wave-length and low-frequency perturbations, the linearised equations reduce to the following dispersion relation:

$$\tilde{\omega}^2 + i\tilde{\omega}(\omega_c + \omega_{th}) - \frac{k_t^2}{k^2} \omega_{BV}^2 = 0, \quad (4)$$

where  $\tilde{\omega} \equiv \omega - k_r v$  is the frequency experienced by a perturbation that rides with the background flow and  $k^2 = k_r^2 + k_t^2$ . In the equation above

$$\omega_c \equiv \frac{\gamma - 1}{\gamma} \frac{k^2 f \kappa_S T^{7/2}}{p}, \quad (5)$$

$$\omega_{th} \equiv -\frac{\gamma - 1}{\gamma} \frac{n \Lambda(T) \Delta(T)}{k_B T}, \quad (6)$$

where  $n = \rho/\mu m_p$  is the particle number density,

$$\Delta(T) \equiv 2 - \frac{d \ln \Lambda}{d \ln T}, \quad (7)$$

and  $\omega_{BV}$  is Brunt-Väisälä (hereafter BV) frequency defined as

$$\omega_{BV} \equiv \left\{ \frac{g}{T} \left[ \frac{dT}{dr} - \left( \frac{dT}{dr} \right)_{\text{adiab}} \right] \right\}^{1/2}$$

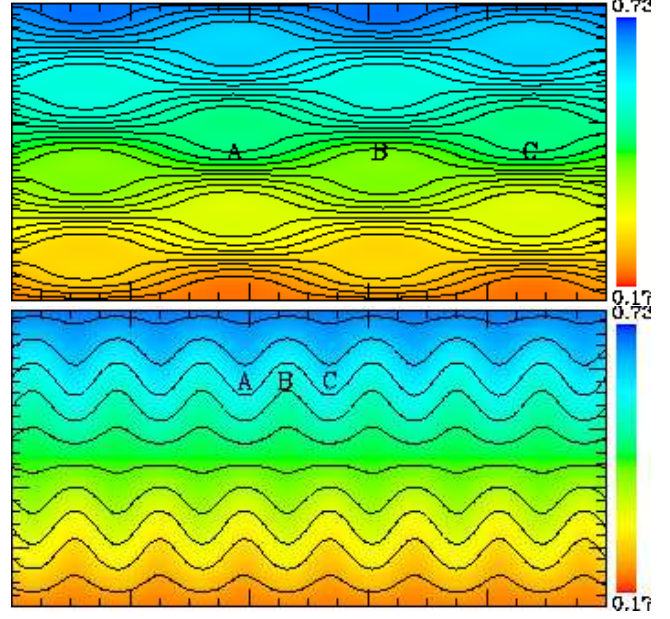


**Figure 1.** Contours of constant specific entropy (in the plane of the tangential and radial coordinates) for a model corona with perturbations that have  $k_t/k_r = 2/7$  (upper panel) and  $7/2$  (lower panel). The gravitational field is directed from top to bottom. Specific entropy is in arbitrary units.

$$= \left[ \frac{g}{T} \left( \frac{dT}{dr} + \frac{\gamma - 1}{\gamma} \frac{g \mu m_p}{k_B} \right) \right]^{1/2}, \quad (8)$$

where  $g = \|\nabla\Phi\|$  and  $(dT/dr)_{\text{adiab}}$  is the adiabatic temperature gradient. The BV frequency  $\omega_{BV}$  is clearly real in the relevant case of convectively stable configurations.

In the absence of cooling and thermal conduction ( $\omega_c = \omega_{th} = 0$ ), the dispersion relation (4) yields

$$\tilde{\omega} = \frac{k_t}{k} \omega_{BV}. \quad (9)$$

Thus  $\omega_{BV}$  is the frequency at which radially-oriented needles of gas bob up and down around their equilibrium radii. As  $k_t/k$  falls from unity, the shape of the oscillating region flattens through a sphere, reaching a tangentially oriented disc in the limit  $k_t/k \rightarrow 0$  (Fig. 1). According to equation (9), the oscillation frequency declines from  $\omega_{BV}$  to zero as the body is flattened from a needle to a disc. To understand this result physically, consider the upper panel of Fig. 1, showing isoentropy contours for a model corona with perturbations that have  $k_t/k_r = 2/7$ . In the absence of cooling or conduction, specific entropy is unchanged as the fluid moves, so the colours and contours are frozen into the fluid. At the points marked A and C in the figure, the entropy perturbation is positive because the fluid is displaced downward from equilibrium, while at point B the fluid is displaced upwards. The upward movement of the contour above B has clearly been enabled by fluid moving away horizontally towards the points A and C. In the lower panel – showing isoentropy contours for the same model corona, but with  $k_t/k_r = 7/2$  – it is clear that the upward movement at B requires a less significant horizontal movement of fluid. Consequently, the effective inertia that has to be overcome by the perturbation's buoyancy increases with the flattening of the perturbation, so  $\tilde{\omega}$  decreases with  $k_t/k$ .

In the absence of conduction or a confining gravitational force ( $\omega_c = \omega_{BV} = 0$ ) equation (4) states that  $\tilde{\omega} = -i\omega_{th}$ , so the flow is unstable when  $\omega_{th} < 0$  (Field 1965). From equation (6)  $\omega_{th} < 0$  when  $\Delta(T) > 0$ , which is always the case at temperatures  $\gtrsim 7 \times 10^4$  K, as is apparent from Fig. 2, in which  $\Delta(T)$  is plotted for the tabulated cooling function of Sutherland & Dopita (1993), which we adopt throughout the paper. Thus, the condition for thermal instability is satisfied in the temperature range of interest and we can specialise to the case  $\omega_{th} < 0$ . The conduction frequency  $\omega_c > 0$  always, and conduction replaces the Field instability with exponential decay when  $\omega_c > |\omega_{th}|$ . Since  $\omega_c \propto k^2$ , the shortest-wavelength modes are always damped.

In the course of buoyant oscillations, a parcel of gas is half the time overdense and cooler with respect to its surroundings, and half the time underdense and warmer, so unless  $|\omega_c + \omega_{th}| \gtrsim (k_t/k)\omega_{BV}$ , neither conduction nor radiation will have a big impact on buoyant oscillations. This expectation is borne out by exact analysis of the dispersion relation (4), which shows that when  $\omega_c = 0$  modes are monotonically growing if  $k_t/k$  is smaller than

$$\left(\frac{k_t}{k}\right)_{\text{crit}} \equiv \frac{|\omega_{th}|}{2\omega_{BV}}. \quad (10)$$

In addition, thermal conduction stabilises perturbations with wavelengths smaller than

$$\lambda_{\text{crit}} \equiv \frac{2\pi}{n} \left[ \frac{f\kappa_S T^{7/2}}{\Lambda(T)\Delta(T)} \right]^{1/2}. \quad (11)$$

Although sufficiently flattened perturbations can be thermally unstable, equation (11) places a lower bound on the thickness of any thermally unstable disc, so such a disc's transverse size must be considerable. It is likely that the hot atmospheres of galaxies, galaxy groups and clusters are turbulent by virtue of cosmic infall, galactic winds and jets from AGN. Consequently, an extended disc-like overdensity is unlikely to remain flat and exactly tangentially oriented for more than a dynamical time. Once turbulence has distorted and/or rotated a perturbation, its value of  $\tilde{\omega}$  will rise towards  $\omega_{BV}$  and it will cease to be thermally unstable. Therefore we can discount the possibility that  $\tilde{\omega} \ll \omega_{BV}$ .

## 2.2 Physical implications

The thermal and dynamical evolution of a galactic corona is ultimately determined by four timescales: the dynamical time of the system  $t_{\text{dyn}}$ , the gas isobaric cooling time

$$t_{\text{cool}} \equiv \frac{\gamma}{\gamma - 1} \frac{k_B T}{n\Lambda(T)}, \quad (12)$$

the BV time  $t_{BV} \equiv \omega_{BV}^{-1}$  and the thermal instability time  $t_{th} \equiv |\omega_{th}^{-1}|$ . Figure 3 illustrates this by plotting these timescales for a particular atmosphere representative of those of massive elliptical galaxies (model HM of Nipoti & Binney 2007, with metallicity  $Z = 0.3Z_\odot$ ; see also Table 1). Clearly, a necessary condition for a corona to be in equilibrium is  $t_{\text{dyn}} < t_{\text{cool}}$ , so in Fig. 3 the dotted line lies above the short-dashed line: a plasma in which this condition is violated is experiencing a cooling catastrophe, and the question of its thermal stability is meaningless. Let us focus on systems with  $t_{\text{dyn}} < t_{\text{cool}}$ , which are approximately in equilibrium and, at least in principle, can be prone to thermal

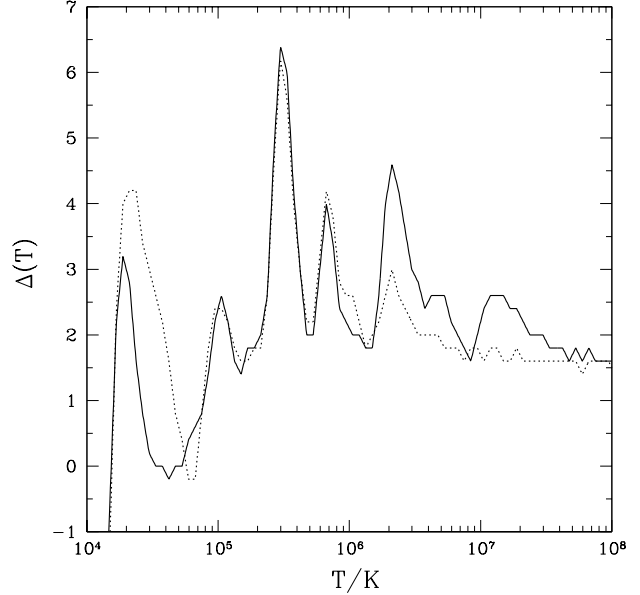


**Figure 2.** The quantity  $\Delta(T) = 2 - d \ln \Lambda / d \ln T$  as a function of temperature (full line:  $Z = Z_\odot$ , dotted curve  $Z = 0.03Z_\odot$ ) for the cooling function of Sutherland & Dopita (1993).

instability. As we have seen, thermal perturbations of average shape ( $k_t \sim k_r$ ) can grow only if  $t_{th} < t_{BV}$ , because otherwise buoyancy is effective in restoring the unperturbed entropy profile. In the typical case of subadiabatic temperature profile, the BV time is of the order of the dynamical time (both being determined mainly by the gravitational field), while the thermal instability time is of the order of the cooling time (both being determined mainly by the cooling function). Hence in Fig. 3 the long-dashed line lies close to the short-dashed line, while the solid line lies close to the dotted line, which necessarily lies above the short-dashed line. As a consequence, it is not easy to find systems in which both the conditions  $t_{\text{dyn}} < t_{\text{cool}}$  and  $t_{th} < t_{BV}$  are satisfied, and this is the main reason why stratified atmospheres are typically thermally stable as MRB pointed out in the context of rich galaxy clusters.

However, from equations (6) and (12),

$$\frac{t_{\text{cool}}}{t_{th}} = |\Delta(T)|, \quad (13)$$

and Fig. 2 shows that  $t_{th} < t_{\text{cool}}$  for  $T \gtrsim 8 \times 10^4$  K. Consequently, for certain temperature and density distributions within the system,  $t_{BV}$  can be longer than  $t_{th}$ , and  $t_{\text{dyn}}$  shorter than  $t_{\text{cool}}$ , even when  $t_{BV} \sim t_{\text{dyn}}$ . Figure 2 shows that the scope for simultaneously satisfying both conditions is largest at temperatures  $\sim 3 \times 10^5$  K where the cooling function increases steeply for decreasing temperature. Thus, the development of thermal instability in galactic coronae, which have virial temperatures in this range, cannot be excluded a priori.

As the temperature profile approaches the adiabatic temperature profile,  $t_{BV}$  becomes arbitrarily long (see equation 8) – in an adiabatic atmosphere there is no tendency for buoyancy to restore displaced material to its original radius. Hence an atmosphere with a very shallow entropy

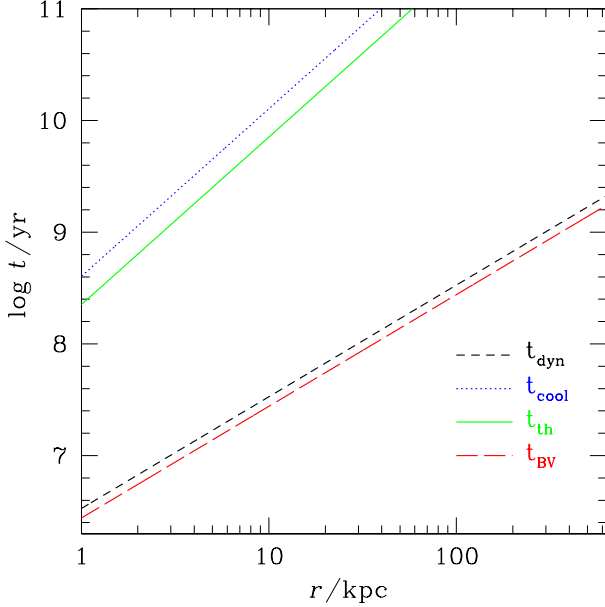


**Figure 3.** The radial dependence of dynamical, cooling, thermal instability and BV timescales in a model atmosphere representative of those of massive elliptical galaxies (model HM of Nipoti & Binney 2007, see also Table 1).

profile may well be thermally unstable. Information on the entropy profile of galactic coronae is then crucial for the issue of their thermal stability (see also BS).

Finally, thermal conductivity can potentially give an important contribution to the suppression of small-scale perturbations: conductivity damps all perturbations with wavelength smaller than the critical wavelength  $\lambda_{\text{crit}}$  (equation 11). The extent of this damping depends on the poorly constrained suppression of conductivity, which we parametrise with the dimensionless factor  $f$ . However, we will see that even strongly suppressed thermal conduction can have non-negligible stabilising effect.

The discussion above leads to the conclusion that the window for the development of thermal instability in galactic coronae is narrow, but not necessarily closed. Thus, to address the question of the thermal stability of the WHIM it is necessary to apply the results of the perturbation analysis to specific models of galactic coronae.

### 3 APPLICATIONS TO GALACTIC CORONAE

Application of the thermal instability analysis to the X-ray emitting hot atmospheres of massive elliptical galaxies and clusters of galaxies has shown clearly that these systems cannot develop thermal instabilities (MRB, BS). This result is apparent from Fig. 3, which shows the relevant timescales for a massive elliptical galaxy model: in this case the BV timescale is at least two orders of magnitude shorter than the thermal instability timescale.

Here we address directly the question of whether the WHIM surrounding disc galaxies is prone to thermal instability. Unfortunately, the properties of the coronae of disc galaxies are not as well known as those of their more massive

counterparts, mainly because they have low X-ray surface brightnesses on account of their low gas densities. Despite various attempts to detect in X-rays the coronae of disc galaxies, so far only upper limits on their X-ray luminosity have been obtained (e.g. Rasmussen et al. 2009). In the cases in which extra-planar X-ray emission is detected, it appears clumpy, with clear connections with the star-forming regions, and is likely to be explained by galactic fountains (e.g. Strickland et al. 2004; Li et al. 2006). But also from these data we can derive upper limits to the total luminosity of the hot halos. In the special case of the Milky Way different pieces of information can be used to constrain the physical properties of the corona (e.g. Fukugita & Peebles 2006).

Here we consider simple non-rotating spherical models of coronae representative of the WHIM surrounding specific disc galaxies, whose gross properties are consistent with the observational constraints. The neglect of rotation is a serious limitation of this work because rotation must become dynamically important sufficiently close to the disc if the corona is to feed the disc. Results for non-rotating coronae are of interest because the clouds we wish to understand lie far from the disc where rotation is expected to be a small effect dynamically, and linear analysis of a differentially rotating coronae is a challenging problem.

The hot gas is in hydrostatic equilibrium with polytropic distribution  $p(r) \propto [\rho(r)]^{\gamma'}$ , where  $\gamma'$  is the polytropic index: the gas temperature profile is

$$\frac{T(r)}{T_0} = 1 - \frac{\gamma' - 1}{\gamma'} \frac{\mu m_p}{k_B T_0} (\Phi - \Phi_0), \quad (14)$$

where  $T_0 \equiv T(r_0)$ ,  $\Phi_0 \equiv \Phi(r_0)$  and  $r_0$  is a reference radius – in the following we assume  $r_0 = 10$  kpc. When  $\gamma' > 1$  the electron number density profile is

$$\frac{n_e}{n_{e,0}} = \left( \frac{T}{T_0} \right)^{1/(\gamma'-1)}, \quad (15)$$

where  $n_{e,0} \equiv n_e(r_0)$  and  $n_e = 0.52n$  (assuming abundances by mass  $Y = 0.25$ ,  $X = 0.75$ ). When  $\gamma' = 1$  the distribution is isothermal at temperature  $T_0$  and the electron density profile is

$$n_e(r) = n_{e,0} \exp \left[ -\frac{\mu m_p}{k_B T_0} (\Phi - \Phi_0) \right]. \quad (16)$$

The gravitational potential  $\Phi$  is determined by the total mass density distribution  $\rho_{\text{dyn}}$ , so  $\nabla^2 \Phi = 4\pi G \rho_{\text{dyn}}$ . The dynamical time is

$$t_{\text{dyn}}(r) \equiv \sqrt{\frac{3\pi}{16G\bar{\rho}_{\text{dyn}}}} = \frac{\pi}{2} \frac{r^{3/2}}{\sqrt{GM_{\text{dyn}}(r)}}, \quad (17)$$

where  $M_{\text{dyn}}(r) = 4\pi \int_0^r \rho_{\text{dyn}}(r') r'^2 dr'$  is the dynamical mass of the system and  $\bar{\rho}_{\text{dyn}} = 3M_{\text{dyn}}(r)/4\pi r^3$  is the average mass density within  $r$ .

We assume here that the total density distributions of our model galaxies follow the singular isothermal sphere

$$\rho_{\text{dyn}}(r) = \frac{k_B T_{\text{vir}}}{2\pi G \mu m_p r^2}, \quad (18)$$

and that the gravitational potential is

$$\Phi(r) = 2 \frac{k_B T_{\text{vir}}}{\mu m_p} \ln \left( \frac{r}{r_0} \right) + \Phi_0, \quad (19)$$

where  $T_{\text{vir}}$  is the virial temperature, which can be linked to the galaxy's circular speed  $v_c$ :

$$T_{\text{vir}} = \frac{\mu m_p}{2k_B} v_c^2. \quad (20)$$

When the gas is isothermal ( $\gamma' = 1$ ) in equilibrium in the potential of a singular isothermal sphere, the gas density distribution reduces to the simple power law

$$n_e(r) = n_{e,0} \left( \frac{r}{r_0} \right)^{-\alpha}, \quad (21)$$

where  $\alpha = 2T_{\text{vir}}/T_0$ .

In summary, each galaxy model is characterised by five parameters:  $T_{\text{vir}}$ ,  $\gamma'$ ,  $T_0$ ,  $n_{e,0}$  and the metallicity  $Z$ , which enters the calculation of the cooling function.

### 3.1 Observational constraints

We use three galaxies as raw models for three categories of galaxies with different masses. The first is NGC 5746, a very massive spiral with flat rotational speed  $\simeq 310 \text{ km s}^{-1}$  (corresponding to a virial temperature  $T_{\text{vir}} \simeq 3.4 \times 10^6 \text{ K}$ ; Rand & Benjamin 2008), for which we take from Rasmussen et al. (2009) the upper limit on the X-ray luminosity of the corona  $L_X < 4 \times 10^{39} \text{ erg s}^{-1}$ . The second is the Milky Way, whose corona is constrained observationally as in Fukugita & Peebles (2006). The third galaxy is NGC 6503, a low-mass spiral seen at an inclination of about 75 degrees, for which *Chandra* observations yield an upper limit  $L_X < 1.6 \times 10^{38} \text{ erg s}^{-1}$  to the X-ray halo luminosity (Strickland et al. 2004). For this galaxy we use  $v_c = 120 \text{ km s}^{-1}$  (Begeman 1987), which by equation (20) leads to a virial temperature  $T_{\text{vir}} = 5.1 \times 10^5 \text{ K}$ . In both NGC 5746 and in NGC 6503 a component of extraplanar neutral gas has been detected (Rand & Benjamin 2008; Greisen, Spekkens & van Moorsel 2009).

For each galaxy we consider an isothermal ( $\gamma' = 1$ ) and an adiabatic corona model ( $\gamma' = \gamma$ ). We verify that the models are consistent with observational constraints by computing their X-ray luminosities using the Mekal recipe (Liedahl, Osterheld & Goldstein 1995) embedded in XSPEC. The 0.3–2 keV fluxes are calculated for a range of gas temperatures ( $0.1 < T < 1.5 \text{ keV}$ ) and for different metallicities ( $Z$ ). Given  $f_{\Delta E}(T, Z)$  the computed specific flux, where  $\Delta E = 0.3 - 2 \text{ keV}$ , the plasma luminosity can be derived as

$$L_{\Delta E}(T, Z) = 10^{-14} \int dV n_e n_H f_{\Delta E}(T, Z) \text{ erg s}^{-1} \text{ cm}^{-3} \quad (22)$$

where  $n_e$  is the electron density and  $n_H$  is the hydrogen density. The factor in front the r.h.s. derives from the XSPEC normalization. For isothermal models the temperature in equation (22) is constant with  $r$  and so is  $f_{\Delta E}(T, Z)$ , so one only integrates  $n_e^2(r)$ , assuming a constant  $n_H/n_e$  ratio. For adiabatic models, the temperature varies with  $r$  and  $f_{\Delta E}(T, Z)$  has to be computed at each  $r$ .

The isothermal model of NGC 5746 has total halo luminosity  $L_X = 3.99 \times 10^{39} \text{ erg s}^{-1}$  in the range  $5 < r < 40 \text{ kpc}$ , consistent with the upper limit on the X-ray luminosity (Rasmussen et al. 2009). Our isothermal model of the Milky Way is very similar to “model 2” of Fukugita & Peebles (2006). We checked that the obtained luminosity is in agreement with observational constraints on galaxies similar to

the Milky Way, for instance NGC 891 (Strickland et al. 2004), which happens to be the case. For the isothermal model of NGC 6503, we assume  $n_{e,0} = 1 \times 10^{-3} \text{ cm}^{-3}$ , which gives a luminosity that matches the upper limit by Strickland et al. (2004). Similarly, the adiabatic models of the three galaxies are constructed so that their X-ray luminosities are consistent with observations.

In contrast to the isothermal case, an adiabatic atmosphere has a sharp edge and a well defined mass. The location of the corona's edge and thus the total gas mass depend strongly on the reference gas temperature  $T_0$ . We find that using the same  $T_0$  (temperature at  $r = 10 \text{ kpc}$ ) as the isothermal models leads to gas masses which are one or two orders of magnitude lower than what is expected for a WHIM corona. Lacking constraints on the temperature profiles, for the Milky Way corona we choose  $T_0$  and  $n_{e,0}$  as the largest values (in order to increase the mass of the corona) that do not conflict with the luminosity constraints: these values, shown in Table 1, give a total WHIM mass of  $\sim 1.3 \times 10^{11} M_\odot$ , in line with the cosmological predictions. For NGC 5746 and NGC 6503 we keep the same ratio between  $T_0$  and  $T_{\text{vir}}$  as for the adiabatic Milky Way model (i.e. same cut-off radius  $\sim 350 \text{ kpc}$ ), maximise  $n_{e,0}$  according to the X-ray luminosity constraints and find total masses of the same order (see rightmost column of Table 1). The density and temperature profiles of our models are shown, respectively, in the first and second rows of panels of Fig. 4 (isothermal models) and Fig. 5 (adiabatic models). The values of the parameters for all models are summarised in Table 1.

## 4 RESULTS

### 4.1 Isothermal coronae

Consider first coronae with isothermal gas distributions ( $\gamma' = 1$ ), which are known to provide reasonable approximations to the hot atmospheres of elliptical galaxies and galaxy clusters. In Fig. 4 we plot the results of applying the instability analysis of Section 2.1 to isothermal models of NGC 5746 (model N5746i; left-hand column), the Milky Way (model MWi; central column) and NGC 6503 (model N6503i; right-hand column). The panels in the third row of Fig. 4 are the analogues of Fig. 3 and show as functions of radius the dynamical, cooling, thermal instability and BV timescales. We see that in all cases  $t_{\text{BV}}$  (long-dashed line) is shorter than  $t_{\text{th}}$  (solid line), and the ratio  $t_{\text{th}}/t_{\text{BV}}$  is higher in galaxies with higher virial temperatures. Hence in all cases the growth of thermal perturbations is effectively countered by buoyancy.

A more detailed analysis of the behaviour of the perturbations can be obtained from the bottom row of panels in Fig. 4, which show as a solid line the maximum wavenumber ratio  $(k_t/k)_{\text{crit}}$  a perturbation can have and still grow monotonically: more tangentially elongated modes [those with  $k_t/k > (k_t/k)_{\text{crit}}$ ] are overstable. In all cases  $(k_t/k)_{\text{crit}}$  is significantly smaller than unity: this means that it is impossible for such an atmosphere to form blobs (i.e., perturbations with  $k_r \sim k_t$  or  $k_t/k \sim 1/\sqrt{2}$ ) by thermal instability. Consistent with the behaviour of the timescales,  $(k_t/k)_{\text{crit}}$  increases for decreasing virial temperature of the system, being  $\lesssim 0.007$  in model N5746i and  $0.06 - 0.25$  in model N6503i.

**Table 1.** Parameters of the model galaxies.  $T_{\text{vir}}$ : virial temperature.  $\gamma'$ : polytropic index.  $T_0$ : electron temperature at  $r = 10$  kpc.  $n_{e,0}$ : electron number density at  $r = 10$  kpc.  $Z$ : metallicity.  $L_X$ : X-ray luminosity.  $M_{\text{gas}}$ : corona gas mass. Isothermal and adiabatic disc galaxy models have names ending with “i” and “a”, respectively. HM is an isothermal corona model representative of a high-mass elliptical galaxy.

Model	$T_{\text{vir}}$ ( $10^6$ K)	$\gamma'$	$T_0$ ( $10^6$ K)	$n_{e,0}$ ( $10^{-3} \text{ cm}^{-3}$ )	$Z$ ( $Z_{\odot}$ )	$L_X(1 < r < 10 \text{ kpc})$ ( $10^{39} \text{ erg s}^{-1}$ )	$L_X(10 < r < 100 \text{ kpc})$ ( $10^{39} \text{ erg s}^{-1}$ )	$M_{\text{gas}}(r < 350 \text{ kpc})$ ( $10^{11} M_{\odot}$ )
HM	7.5	1	10	3.5	0.3	91.56	91.56	1.7
N5746i	3.4	1	5.4	1.2	0.03	2.11	6.67	1.22
MWi	1.4	1	1.9	2.6	0.03	4.64	5.33	1.36
N6503i	0.51	1	0.82	1	0.03	0.04	0.13	1.01
N5746a	3.4	5/3	9.7	0.62	0.03	0.27	12.88	1.23
MWa	1.4	5/3	4	0.68	0.03	0.19	5.58	1.30
N6503a	0.51	5/3	1.45	0.5	0.03	0.03	0.22	0.96

Thus, very tangentially elongated disturbances can in principle grow, but we have seen that we do not expect them to grow in practice (see Section 2.1). The next-to-bottom row of Fig. 4 quantifies ability of thermal conduction to stop growth by showing the critical wavelength  $\lambda_{\text{crit}}$  as a function of radius (solid line). Studies of galaxy clusters indicate that a realistic value of the thermal conduction suppression factor is  $f \sim 0.01$  (Nipoti & Binney 2004, and references therein), and in this case at a radius  $r$  all perturbations smaller than  $\sim 0.1r$  in extent are damped in the Milky-Way model MWi. Stabilisation by thermal conduction is proportionally more effective in higher-temperature systems than in lower-temperature systems. For instance, in NGC 5746 at all radii perturbations with wave-length smaller than the system’s radius are damped for  $f = 0.01$ , while this is not the case in NGC 6503.

We conclude that if galactic coronae are isothermal, the growth of thermal perturbations is effectively suppressed by buoyancy and thermal conduction. Suppression is particularly strong in very massive systems such as NGC 5746, but it is very effective also in coronae of Milky-Way-like galaxies and smaller. All these systems are unlikely to form cold clouds by thermal instability.

## 4.2 Polytropic coronae

Though isothermality is a well motivated assumption, we cannot exclude the possibility that galactic coronae have shallower specific entropy profiles, so in this section we investigate coronae in which the polytropic relation  $p(r) \propto [\rho(r)]^{\gamma'}$  holds between pressure and density. As  $\gamma'$  ranges from unity to  $\gamma = \frac{5}{3}$ , these coronae range from isothermal to adiabatic.

The results for the adiabatic models (N5746a, MWa and N6503a in Table 1) are shown in Fig. 5. The cooling and thermal instability timescales are now not power-law functions of radius because density and temperature are no longer power-law functions as in the isothermal models (see first and second rows of panels). In an adiabatic atmosphere there is no buoyancy to counter the growth of thermal instability, so all modes with  $\lambda > \lambda_{\text{crit}}$  grow monotonically, independent of their wavenumber ratio [ $t_{\text{BV}} \rightarrow \infty$  and  $(k_t/k)_{\text{crit}} \rightarrow \infty$ ]. Thus the thermal stability of the gas is determined by the critical wavelength  $\lambda_{\text{crit}}$ , which is shown in the bottom row of panels in Fig. 5. If the thermal conduction suppression factor is  $f = 0.01$ , perturbations are effectively stabilised in

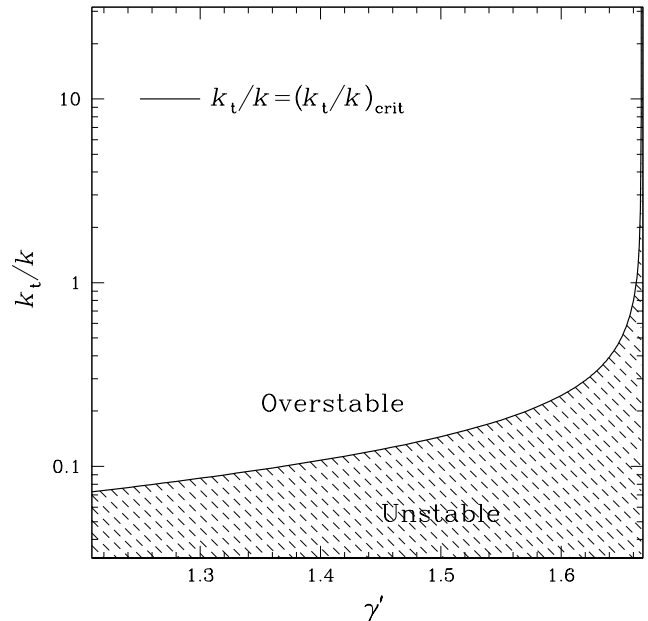


**Figure 6.** Critical wavenumber ratio  $(k_t/k)_{\text{crit}}$  as a function of the polytropic index  $\gamma'$  at the half-mass radius  $r_{\text{half}}$  for Milky-Way-like polytropic models with  $T_{\text{vir}} = 1.4 \times 10^6$  K and  $Z = 0.03Z_{\odot}$ .

model N5746a, but not as much in models MWa and N6503a. Thus, thermal instabilities cannot develop in the corona of NGC 5746, even if it has an adiabatic distribution of gas. In the case of the Milky Way, perturbations smaller than  $\sim 10$  kpc in size are expected to be stabilised by thermal conduction for  $r \lesssim 200$  kpc. In the case of NGC 6503 perturbations smaller than 2.5 kpc in size are stable for  $r \lesssim 100$  kpc. However, if the coronae of lower-mass systems such as the Milky Way and NGC 6503 have adiabatic distributions of gas, the growth of sufficiently large perturbations by thermal instability is not excluded at large radii. The rightmost panel in the third row of Fig. 5 indicates that at  $r \gtrsim 150$  kpc in model N6503a the perturbation analysis does not apply because at these radii  $t_{\text{cool}} \lesssim t_{\text{dyn}}$  so the corona is not in hydrostatic equilibrium; catastrophic cooling is occurring.

The assumption of perfectly adiabatic atmosphere is quite extreme, so it is natural to explore the thermal insta-



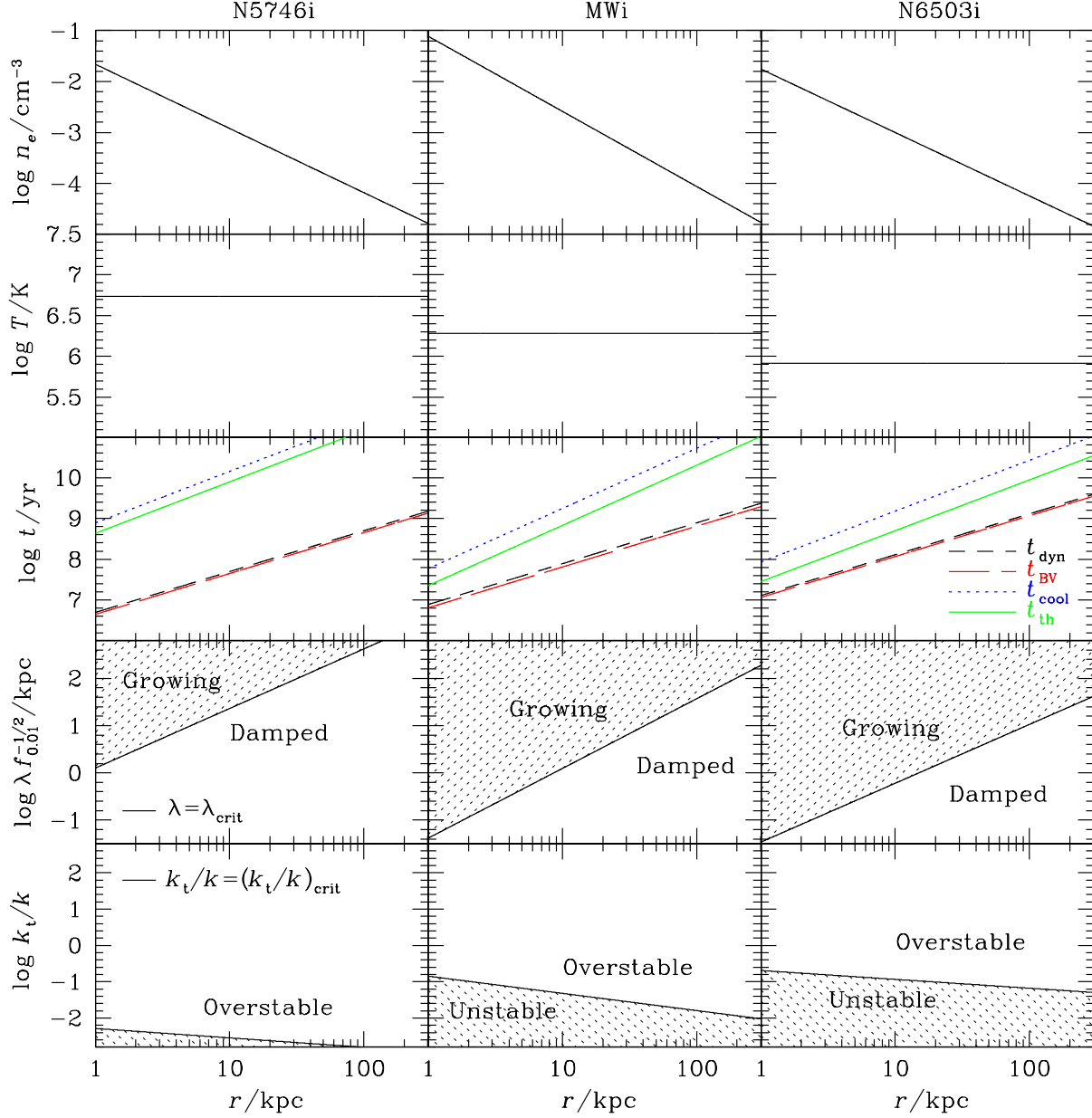


**Figure 4.** From top to bottom: electron density, temperature, timescales, perturbation wavelength, and tangential-to-total perturbation wavenumber ratio as functions of radius for the isothermal models N5746i (left-hand column), MWi (central column) and N6503i (right-hand column). The timescales panels plot the dynamical (short dashed), BV (long dashed), cooling (dotted) and thermal instability (solid) timescales. In the wavelength panels the solid curves represent the critical wavelength  $\lambda_{\text{crit}}$  for stabilisation by thermal conduction: only perturbations with wavelengths in the shaded areas grow ( $f$  is the factor by which thermal conduction is suppressed; see equation 3). In the wavenumber ratio panels the solid curves represent the critical wavenumber ratio  $(k_t/k)_{\text{crit}}$  for instability: only perturbations with ratio in the shaded areas are unstable.

bility of corae with entropy profiles intermediate between the steep ones of isothermal models and the perfectly flat ones of adiabatic models. For this purpose we consider polytropic models with  $1 < \gamma' < \gamma$ . For a polytropic distribution with index  $\gamma'$  the BV frequency is

$$\omega_{\text{BV}}^2 = \frac{g^2}{T} \frac{\mu m_p}{k_B} [h(\gamma, \gamma')]^2, \quad (23)$$

where

$$h(\gamma, \gamma') \equiv \left( \frac{1}{\gamma'} - \frac{1}{\gamma} \right)^{1/2}. \quad (24)$$

Thus we obtain the following expression for the maximum ratio of wavenumbers that is consistent with growing mode:



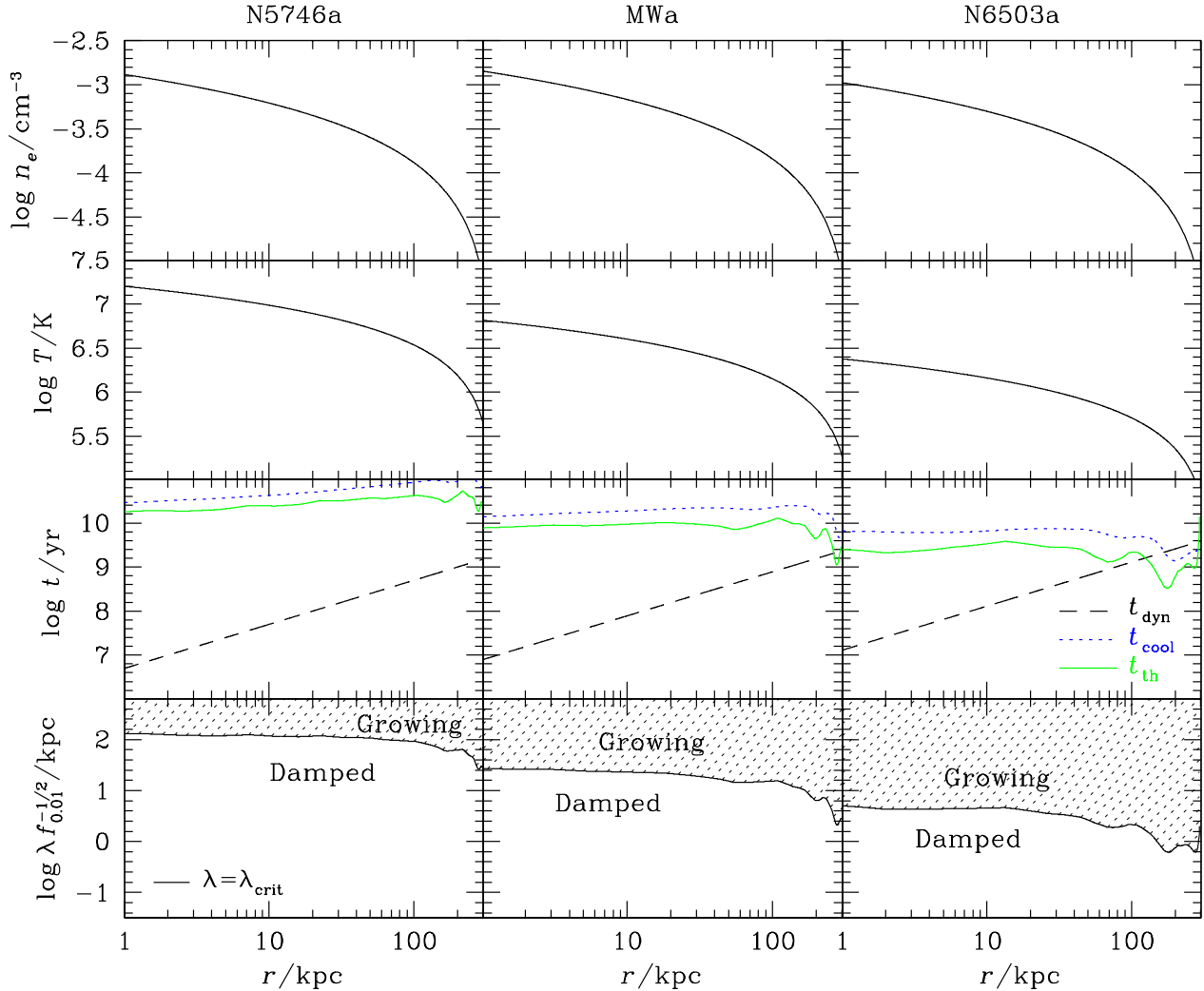


**Figure 5.** Same as Fig. 4 but for the adiabatic models N5746a (left-hand column), MWa (central column) and N6503a (right-hand column). In these cases  $t_{\text{BV}}$  and  $(k_t/k)_{\text{crit}}$  are infinite at all radii, so we do not plot diagrams of  $k_t/k$ .

$$\left(\frac{k_t}{k}\right)_{\text{crit}} = \frac{\gamma - 1}{2\gamma h(\gamma, \gamma')} \frac{n\Lambda(T)\Delta(T)}{(\mu m_p k_B)^{1/2} T^{1/2} g}. \quad (25)$$

We focus on Milky-Way-like polytropic models of index  $\gamma'$ , with  $T_{\text{vir}} = 1.4 \times 10^6$  K,  $Z = 0.03Z_{\odot}$ , and values of  $n_{e,0}$  and  $T_0$  such that they have the same gas mass within 500 kpc and the same value of the specific entropy at the radius  $r_{\text{half}}$  containing half of the gas mass as the adiabatic model MWa. In Fig. 6 we plot as a solid line  $(k_t/k)_{\text{crit}}$  as a function of  $\gamma'$  at  $r = r_{\text{half}}$ , which is in the range 140 – 170 kpc for these models. Only perturbations with  $k_t/k < (k_t/k)_{\text{crit}}$  (shaded area in the diagram) are unstable. We see that as soon as  $\gamma'$  deviates from  $\gamma$ ,  $(k_t/k)_{\text{crit}}$  drops from infinity to values smaller than unity, and  $(k_t/k)_{\text{crit}} \lesssim 0.2$  for  $\gamma' \lesssim 1.55$ . This means that thermal instability is efficiently countered by buoyancy even in polytropic distributions with quite shallow entropy profiles. We conclude that unless the Milky Way corona is very close to adiabatic, thermal perturbations cannot grow.

### 4.3 Time evolution of polytropic coronae

In the absence of strong observational constraints, we try here to address on theoretical grounds the question of whether the coronae of disk galaxies are close adiabatic by exploring how a corona with a shallow entropy profile evolves in time in the presence of cooling. If a steep outward-increasing entropy profile were produced quickly, we could discard the hypothesis that coronae have very shallow entropy profiles. For this purpose, we consider the extreme case of a corona that starts from a perfectly flat entropy profile ( $\gamma' = \gamma$  polytrope) and the more general case of coronae with shallow outward increasing entropy profiles ( $\gamma' < \gamma$  polytropes).

The left panels in Fig. 7 show how an initially adiabatic model of the corona of the Milky Way evolves over 1 Gyr. Although the central density rises steadily (top left), the temperature profile changes significantly only at the outer edge of the corona (bottom left). Here the temperature was initially  $\lesssim 3 \times 10^5$  K, and, as one moves outwards, the in-

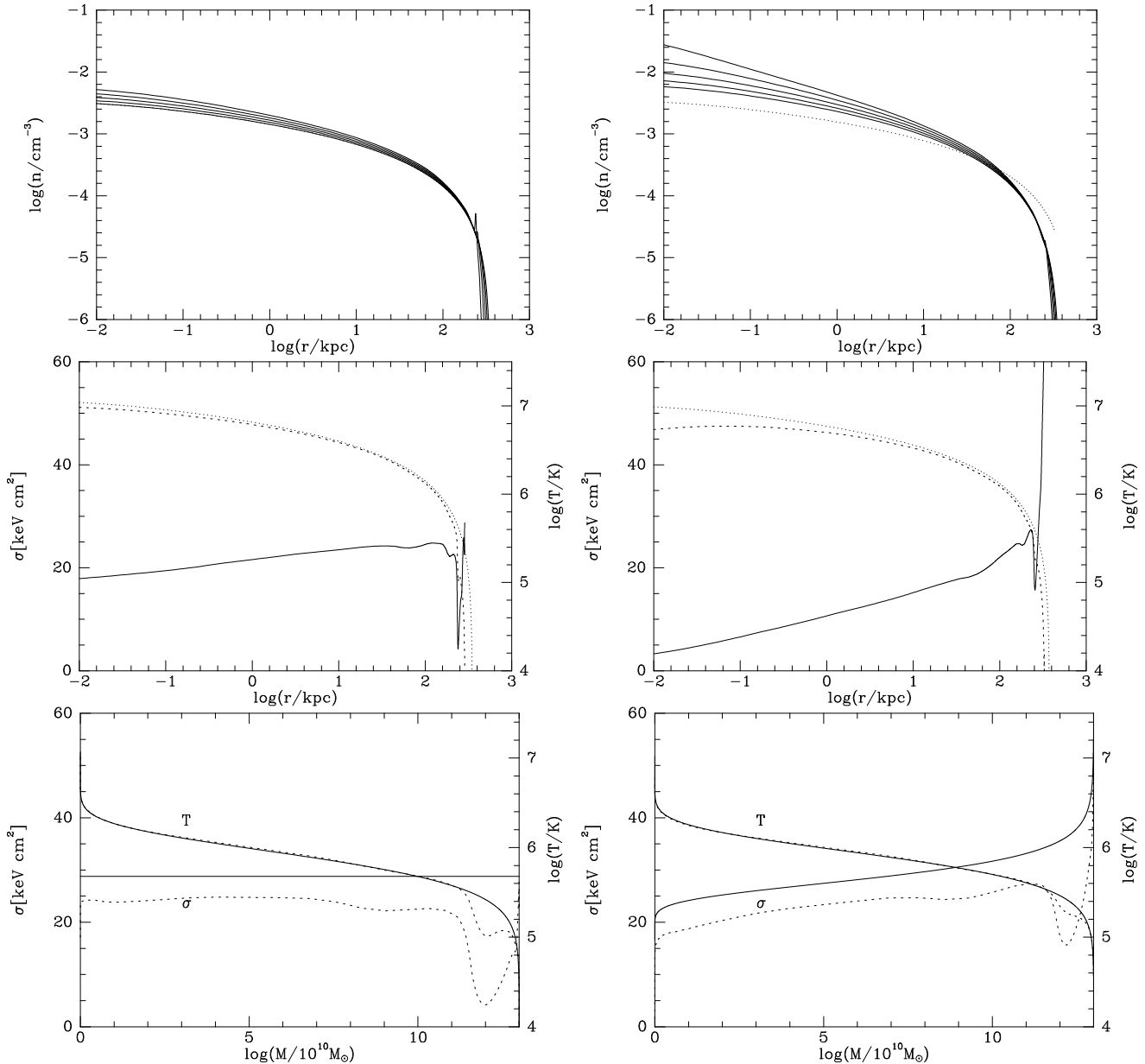


**Figure 7.** Evolution over 1 Gyr of model coronae for the Milky Way. Left column: an initially adiabatic model ( $\gamma' = 1.6667$ ). Right column: a model with  $\gamma' = 1.55$ . The full curves in the top panels show the increase in the central electron density over 1 Gyr, while the dotted curve in the top right panel shows the initial density profile of the adiabatic model of the left column. In the central and bottom panels the left scale gives  $\sigma = p\rho^{-\gamma}$  (in units of  $\text{keV cm}^2$ ) and the right scale gives  $\log T$ . In the central panels the independent variable is radius and broken curves show temperature (the dotted curve shows the initial condition). In the bottom panels the independent variable is mass shell and initial and final conditions are shown by full and dashed curves respectively. The coronae were evolved by the technique described in Kaiser & Binney (2003) with metallicity  $Z = 0.03Z_{\odot}$ .

crease in the efficiency of cooling with falling temperature outweighs the reduction in efficiency with decreasing density. Consequently, the initially flat profile of specific entropy  $\sigma$  starts to fall with radius. In this region of outwards-decreasing specific entropy, the corona is convectively unstable and clouds of cool gas will fall inwards. Further in, the specific entropy profile remains extremely flat as entropy is radiated away, and regions of depressed temperature will not be stabilised by buoyancy. Thus a non-linear computation confirms that in the extreme case of an adiabatic at-

mosphere perturbations large enough not to be damped by thermal conduction can form cool clouds.

It is unlikely that all the corona's gas will have exactly the same specific entropy – initially some gas is bound to have more specific entropy than other gas, and the galaxy's gravitational field will sort the gas by specific entropy such that low-entropy gas lies inside higher-entropy gas. We now address the question of how wide a spread in specific entropy is required to prevent cooling producing a region of outwards-decreasing specific entropy in which clouds could form. A simple way of answering this question is to consider

the cooling of coronae that are initially polytropes of index  $\gamma' < \gamma$ , and we focus here on the Milky-Way-like models of Fig. 6.

The right panels of Fig. 7 show the evolution of the Milky-Way corona that starts from the polytrope with  $\gamma' = 1.55$ . The full curve labelled “ $\sigma$ ” in the bottom right panel shows this corona initially has a significant entropy gradient in the outer region, where an entropy depression formed in the adiabatic case. The dotted curve for  $\sigma$  in the bottom right panel shows that after 1 Gyr, the entropy gradient has been reversed, and there is again a region of outwards-decreasing specific entropy. For polytropic indices  $\gamma' \lesssim 1.4$  a cooling catastrophe develops at the centre before there has been significant cooling at the periphery, and for  $\gamma' = 1.4$  a point of inflection develops in  $\sigma(M)$  at  $M = 12.2 \times 10^{10} M_\odot$  around the time ( $\approx 0.5$  Gyr) when cooling becomes catastrophically fast at the centre.

The central panels of Fig. 7 show that thermal instability occurs only at radii in excess of 100 kpc. This is the case because the steep portion in the cooling curve, which drives the instability, occurs at temperatures that are significantly below the central temperature of the corona – such temperatures are reached only close to the edge of the corona because when the circular speed is assumed constant (as here) they imply a steep density profile. In fact, the formation of a region of outwards-decreasing specific entropy depends sensitively on the shape of the cooling function. When  $\Lambda(T)$  is that given by Sutherland & Dopita (1993) for zero metallicity, no such region forms because  $\Lambda(T)$  does not fall steeply enough with increasing temperature. At zero metallicity an initially adiabatic corona develops an outwards-increasing entropy gradient on account of the increase in the radiation rate with increasing density.

Once entropy is either independent of radius or outwards-decreasing, there is nothing to inhibit bulk radial motion of gas. In an adiabatic atmosphere such motions need to be externally excited, for example by tidal fields and the motion of dark-matter substructures and satellite galaxies as they orbit through the host gravitational potential. In a convectively unstable atmosphere, such motions will arise spontaneously. Radial bulk motions transfer heat between different radial shells of a corona, and, as in the theory of stellar structure, it is natural to assume that convective energy transport will maintain an adiabatic entropy profile in any region in which entropy would otherwise be outwards-decreasing. Hence we modified the code that produced Fig. 7 to include convection as follows. After each timestep, the code looks for regions in which entropy is outwards-decreasing and sets the specific entropy  $s_i = \ln(\sigma) + \text{constant}$  of each mass shell in this region to a common value  $\bar{s}$ . The search for regions of outwards-decreasing entropy, and subsequent entropy adjustment is then repeated until no such region is found. The entropy  $\bar{s}$  is reached as a result of the  $i$ th mass shell receiving an amount of heat  $dq_i$  from the other shells, thus changing its specific entropy by

$$\bar{s} - s_i = ds_i = \frac{dq_i}{T_i M_i}, \quad (26)$$

where  $T_i$  and  $M_i$  are the temperature and mass of the  $i$ th shell. By conservation of energy,  $\sum_i dq_i = 0$ , so after multiplying (26) through by  $T_i M_i$  and summing over  $i$  we have  $\bar{s} = \sum_i s_i T_i M_i / \sum_i T_i M_i$ .

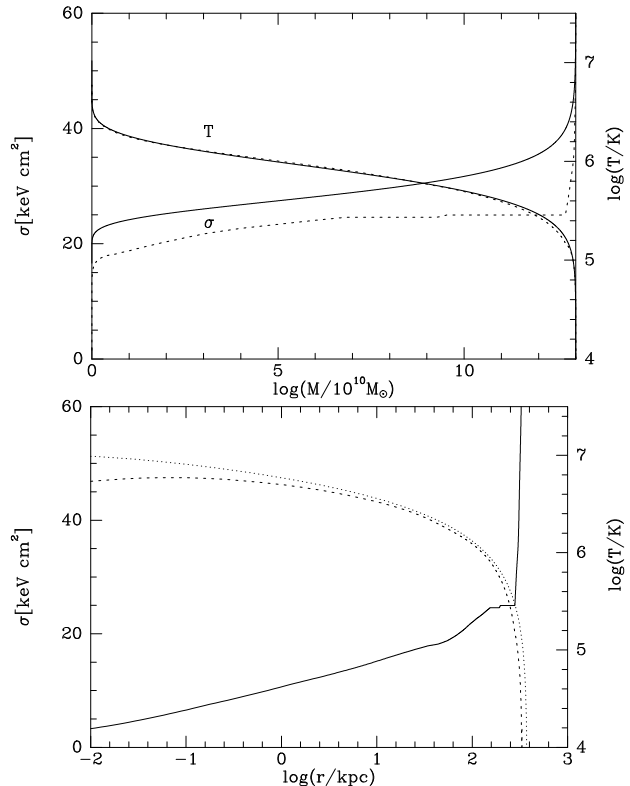


**Figure 8.** The evolution of the initial polytrope with  $\gamma' = 1.55$  when convection is assumed to prevent entropy decreasing outwards. Top panel as a function of mass; lower panel as a function of radius.

Fig. 8 shows the evolution of the initially polytropic corona plotted in the right panels of Fig. 7 when this algorithm is used to simulate the effects of convection. One sees that after a Gyr specific entropy is constant through nearly half the mass. Thus metal-enhanced cooling combined with convection has considerable potential for driving the outer half of a polytropic corona to an adiabatic configuration, provided that the initial entropy profile is shallow enough. However, the fact that polytropic models are characterised by a finite boundary at which the temperature drops to zero is crucial for these systems to evolve towards a configuration with flat entropy profile in the outer regions. We do not expect that these conditions are met in real galaxies, which are surrounded by the intergalactic medium.

## 5 CONCLUSIONS

In this paper we examined the proposal that HVCs of the Milky Way and other disc galaxies form by condensation of the WHIM through thermal instability. The linearised equations for the evolution of thermal perturbations within a cooling, conducting, non-rotating spherical corona show that unless specific entropy is a shallow function of radius (a nearly adiabatic corona), regions in which the temperature is initially anomalously low do not experience the classical Field instability. In fact they are simply points at which an internal gravity wave is momentarily in the ascendant, and after half a Brunt-Väisälä period the material in this region will sink to below its equilibrium radius and will then be an

anomalously warm region. Consequently, there is no thermal instability from which clouds can form in a corona in which there is a significant gradient in the specific entropy.

Clouds can form in a strictly adiabatic corona because in this case buoyancy vanishes and the increase in the specific cooling function  $\Lambda(T)$  with decreasing temperature around  $T \sim 3 \times 10^5$  K can cause the cooling rate to increase outwards notwithstanding the steady decline in gas density with radius. This increase in the cooling rate can cause the specific entropy to become outwards-decreasing and thus the corona to become convectively unstable. In these circumstances clouds of rapidly cooling material will tumble inwards if thermal conductivity is too weak to carry enough heat from the warm interior to the rapidly cooling periphery to offset radiative cooling.

An examination of adiabatic coronae for three galaxies, NGC 5746, the Milky Way, and NGC 6503 shows that thermal conductivity that is suppressed to 1% of Spitzer's fiducial value would eliminate thermal instability entirely in NGC 5746 and largely in the Milky Way, where perturbations smaller than 10 kpc in extent could grow only at  $r \gtrsim 200$  kpc. The efficiency with which thermal conductivity can suppress thermal instability is greatest in the hottest coronae because the Spitzer's conductivity is a strongly increasing function of temperature. So in a low-mass galaxy such as NGC 6503, perturbations 10 kpc in extent could grow through most of the corona, although a perturbation only a kpc in extent would be stabilised almost everywhere.

It is implausible that all the gas in a corona initially has exactly the same specific entropy. The gas will inevitably be spread over a range of specific entropies, and within a few dynamical times convection will sort the corona by specific entropy so that entropy is outwards-increasing. A convenient way of simulating the consequences of such a spread in entropy is to consider coronae that are initially polytropes with index  $\gamma' < \gamma$ . In such coronae there is a significant radial gradient in specific entropy near the corona's edge, where the temperature is low and thermal instability is most likely. Non-linear simulations of the cooling of initially polytropic coronae for the Milky Way show that when the polytropic index  $\gamma'$  is smaller than 1.4, cooling steepens the initial outwards-increasing entropy gradient rather than reversing it and this ensures that anomalously cool regions are buoyantly stabilised against thermal instability.

Our conclusion that a flat entropy profile is a necessary condition for the growth of thermal instability in galactic coronae is consistent with the recent results of SPH simulations by Kaufmann et al. (2009), who find that cold clouds form from hot gas only in systems with flat entropy profiles. However, we find that except in very low-mass systems, thermal conductivity (which was not considered by Kaufmann et al. 2009), is capable of suppressing thermal instability at most radii, even when the conductivity is strongly suppressed.

In light of these results, is it likely that the clouds of H I that are actually observed have formed by cooling of coronal gas? A major issue is that observed H I clouds, such as Complex C and the filament of NGC 891 lie at radii  $\sim 10$  kpc (Oosterloo, Fraternali & Sancisi 2007). Clouds are not found as far out as the bounding radii of a nearly adiabatic atmospheres that would contain the missing baryons, while theory indicates that it is precisely near these radii

that clouds may form as a result of the coronal temperature falling through  $T \simeq 3 \times 10^5$  K, where the cooling function is sufficiently steep. One might speculate that initially clouds have densities and masses that lie below the thresholds for detection, and it is only after they have fallen in to much smaller radii, where the confining pressure is higher, and accreted coronal gas or merged with other clouds, that they become detectable. In this case deeper surveys should find clouds out to in excess of 100 kpc. However, a difficulty with this proposal is that small clouds are thermally unstable only if the corona's thermal conductivity is heavily suppressed – in fact to less than a percent of Spitzer's value.

Thermal instability only occurs if the coronal temperature falls through  $T \simeq 3 \times 10^5$  K. In the polytropic coronae discussed here this condition is satisfied because  $T$  vanishes at a finite radius. However, this feature of a polytropic corona is artificial: in reality the corona will at some point merge into the general intergalactic medium, which is likely to have high entropy and a temperature which could well be above  $5 \times 10^5$  K.

Except in Section 4.3 our analysis is linear in nature and does not apply close to the star-forming disc since this region is violently disturbed by expanding supershells. However, linear analysis should be a reasonable approximation several kiloparsecs from the disc where HVCs are observed.

A significant limitation of our work is that it excludes both magnetic fields and rotation of the corona. Loewenstein (1990) and Balbus (1991) showed that magnetic fields can in principle have a big impact on the stability of cooling flows. However, the relevance of the linear calculations presented by these authors to real cooling flows and coronae is doubtful because in order to perform the analysis one has to assume an unperturbed magnetic-field configuration that is consistent with the unperturbed cooling flow – this field turns out to be radial. The modes obtained obviously reflect the particular stress tensor of this field, and are valid only for perturbations that do not significantly change the field geometry because  $\delta \mathbf{B} \ll \mathbf{B}$ . In cooling flows magnetic pressure is much smaller than thermal pressure and probably on the order of the turbulent pressure  $\rho v_{\text{turb}}^2$ . Consequently the results of Loewenstein (1990) are valid only when the velocities associated with modes are small compared to  $v_{\text{turb}}$ . But we are precisely interested in the turbulent motions themselves, so this condition will be seriously violated. Moreover, given that the magnetic pressure is not larger than the turbulent pressure, the magnetic field will be tangled by the turbulence rather than have the special geometry required by the assumption that a steady state is maintained in the presence of a radial accretion flow. It seems likely that in these circumstances the safest procedure is simply to assume that the effect of the (tangled) magnetic field is confined to augmenting the isotropic pressure by  $\sim B^2/2\mu_0$ . In this case our results are applicable.

Rotation, by contrast, may have a significant impact on thermal stability. Indeed, if clouds that condense from the corona are to feed the growth of a centrifugally supported gas disc, rotation must be dynamically important near the disc. However, clouds are observed far from the disc, where rotation will be less important, and the question is whether a level of rotation that is dynamically small (in the sense that the centrifugal acceleration is much smaller than the gravitational acceleration) can introduce thermal instabil-

ity by obstructing internal gravity waves. We reserve this difficult question for a later paper.

We conclude that, if galactic haloes are well represented by non-rotating, quasi-hydrostatic atmospheres, thermal instability is not a viable mechanism for the formation of cold clouds in disc galaxies as massive as, or more massive than, the Milky Way. It may just work in low-mass systems if their (essentially unconstrained) entropy profiles are almost perfectly flat. Our best guess is that the observed population of HVCs around the Milky Way and other large nearby galaxies represent gas that has been stripped from satellites. This conclusion leaves open the question of how gas moves from the WHIM to the disc, as it must if star formation is to be sustained. Fraternali & Binney (2008) present circumstantial evidence that the key to this transfer is the galactic fountain, which constantly cycles disc gas through the bottom of the corona. To understand this transfer we need models of the corona that include significant centrifugal support near the disc.

## REFERENCES

- Agertz O., et al., 2007, MNRAS, 380, 963  
 Balbus S.A., 1988, ApJ, 328, 395  
 Balbus S.A., 1991, ApJ, 372, 25  
 Balbus S.A., Soker N., 1989, ApJ, 341, 611 (BS)  
 Bell E.F., et al., 2008, ApJ, 680, 295  
 Begeman K.G.B., 1987, *PhD thesis*, University of Groningen  
 Binney J., Cowie L.L., 1981, ApJ, 247, 464  
 Bregman J.N., 1980, ApJ, 236, 577  
 Brüns C., Kerp J., Kalberla P.M.W., Mebold U., 2000, A&A, 357, 120  
 Chiappini C., Matteucci F., Romano D., 2001, ApJ, 554, 1044  
 Cowie L.L., Binney J., 1977, ApJ, 215, 723  
 Ferrara A., Einaudi G., 1992, ApJ, 395, 475  
 Field G.B., 1965, ApJ, 142, 531  
 Fox A., Savage B.D., Wakker B.O., 2006, ApJS, 272, 23  
 Fraternali F., Binney J., 2008, MNRAS, 386, 935  
 Fukugita M., Hogan C.J., Peebles P.J.E., 1998, ApJ, 503, 518  
 Fukugita M., Peebles P.J.E., 2006, ApJ, 639, 590  
 Greisen E.W., Spekkens K., van Moorsel G.A., 2009, AJ, 137, 4718  
 Kaiser C.R., Binney J., 2003, MNRAS, 338, 837  
 Kaufmann T., Mayer L., Wadsley J., Stadel J., Moore B., 2006, MNRAS, 370, 1612  
 Kaufmann T., Mayer L., Wadsley J., Stadel J., Moore B., 2007, MNRAS, 375, 53  
 Kaufmann T., Bullock J.S., Maller A.H., Fang T., Wadsley J., 2009, MNRAS, in press (arXiv:0812.2025)  
 Li Z., Wang Q.D., Irwin J.A., Chaves T., 2006, MNRAS, 371, 147  
 Liedahl D.A., Osterheld A.L., Goldstein W.H., 1995, ApJL, 438, 115  
 Loewenstein M., 1990, ApJ, 349, 471  
 Malagoli A., Rosner R., Bodo G., 1987, ApJ, 319, 632 (MRB)  
 Maller A.H., Bullock J.S., 2004, MNRAS, 355, 694  
 Marri S., White S. D. M., 2003, MNRAS, 345, 561  
 Nipoti C., Binney J., 2004, MNRAS, 349, 1509  
 Nipoti C., Binney J., 2007, MNRAS, 382, 1481  
 Nulsen P.E.J., 1986, MNRAS, 211, 377  
 Oort J.H., 1970, A&A, 7, 381  
 Oosterloo T., Fraternali F., Sancisi R., 2007, AJ, 134, 1019  
 Peek J.E.G., Putman M.E., Sommer-Larsen J., 2008, ApJ, 674, 227  
 Peterson J.R., Kahn S.M., Paerels F.B.S., Kaastra J.S., Tamura T., Bleeker J.A.M., Ferrigno C., Jernigan J.G., 2003, ApJ, 590, 207  
 Price D.J., 2008, JCoPh, 227, 10040  
 Putman M.E., Bland-Hawthorn J., Veilleux S., Gibson B.K., Freeman K.C., Maloney P.R., 2003, ApJ, 597, 948  
 Rand R.J., Benjamin R.A., 2008, ApJ, 676, 991  
 Rasmussen J., Sommer-Larsen J., Pedersen K., Toft S., Benson A., Bower R. G., Grove L. F., 2009, ApJ, 697, 79  
 Richardson J.C., et al., 2008, AJ, 135, 1998  
 Sancisi R., Fraternali F., Oosterloo T., van der Hulst T., 2008, A&ARv., 15, 189  
 Sembach K.R., et al., 2003, ApJS, 146, 165  
 Shapiro P. R., Field G. B., 1976, ApJ, 205, 762  
 Silk J., 1976, ApJ, 208, 646  
 Sommer-Larsen J., 2006, ApJ, 644, L1  
 Spitzer L., 1956, ApJ, 124, 20  
 Spitzer L., 1962, *Physics of Fully Ionized Gases*. Wiley-Interscience, New York  
 Strickland D.K., Heckman T.M., Colbert E.J.M., Hoopes C.G., Weaver K.A., 2004, ApJS, 151, 193  
 Sutherland R.S., Dopita M.A., 1993, ApJS, 88, 253  
 Tribble P.C., 1989, MNRAS, 238, 1  
 Wakker B.P., van Woerden H., 1997, ARA&A, 35, 217  
 Wakker B.P., et al., 2007, ApJ, 670, 113L  
 Westmeier T., Braun R., Thilker D., 2005, A&A, 436, 101  
 White R.E., III, Sarazin C.L., 1987, ApJ, 318, 612